Comparison of a 2.7-mm and 3.5-mm locking compression plate for ulnar fractures: a biomechanical evaluation

Jenna M. Wahbeh, MS[a,b], Benjamin V. Kelley, MD[c], Cyrus Shokoohi, BS[b], Sang-Hyun Park, PhD[a,c], Sai K. Devana, MD[c], Edward Ebramzadeh, PhD[a,c], Sophia N. Sangiorio, PhD[a,b,c,*], Devon M. Jeffcoat, MD[c]

Abstract

Objectives: Implant prominence after ulnar fracture fixation may be mitigated by the use of lower profile plates. The biomechanical strength and stability of 2.7-mm and 3.5-mm locking compression plates for fixation were compared.

Methods: Two fracture conditions, transverse (N = 10) and oblique (N = 10), were evaluated in an in vitro study. Half of the specimens for each condition were fixed with 2.7-mm plates and the other half with 3.5-mm plates, all fixed with conventional dynamic compression mechanisms. Specimens were loaded under ±2 Nm of cyclic axial torsion, then under 10 Nm of cyclic cantilever bending, and bending to failure. Interfragmentary motion and strain were analyzed to determine construct stability as a function of fracture pattern and plate size.

Results: Interfragmentary motion was significantly larger in all constructs fixed with 2.7-mm plates, compared with 3.5-mm plates ($P < 0.01$). The 2.7-mm constructs with transverse fractures had the greatest motion, ranging between 5° and 10° under axial rotation and 5.0–6.0 mm under bending. Motions were the lowest for 3.5-mm constructs with oblique fractures, ranging between 3.2 and 4.2 mm under bending and 2°–3.5° for axial rotation. For oblique fractures, the bending moment at ultimate failure was 31.4 ± 3.6 Nm for the 2.7-mm constructs and 10.0 ± 1.9 Nm for 3.5-mm constructs ($P < 0.01$). Similarly, for transverse fractures, the bending moment was 17.9 ± 4.0 Nm for the 2.7-mm constructs and 9.7 ± 1.3 Nm for the 3.5-mm constructs ($P < 0.01$).

Conclusions: Although 3.5-mm plates were more effective at reducing fracture motion, they were consistently associated with refracture at the distal-most screw hole under load to failure. By contrast, 2.7-mm plates plastically deformed despite excessive loads, potentially avoiding a subsequent fracture.

Level of Evidence: Level V.

Key Words: isolated ulnar shaft fracture, locking compression plate, fracture fixation, 2.7-mm plate, 3.5-mm plate

1. Introduction

Ulnar shaft fractures, both isolated and concomitant with radial shaft fractures, are common traumatic injuries in adults.[1–4] The current standard of care is open reduction and internal fixation using compression plates.[5,6] For simple fracture patterns, anatomic reduction with rigid fixation promotes primary bone healing and enables pronation and supination of the forearm.[7–10] Postoperative surgical complications include loss of reduction, delayed union, and nonunion.[11,12] In addition, given the subcutaneous location of the ulna, the rate of reoperation for implant prominence is high.[13–15] Furthermore, refracture after implant removal is common, reportedly occurring in 11% of patients.[14,16,17] Accordingly, there has been interest in the use of lower profile plates to decrease implant prominence.[10,18,19]

Previous biomechanical studies have assessed the structural stability of ulnar fractures for various conditions affecting mechanical strength of the fracture fixation construct, such as gap size, number and positon of screws, and distance between plate and bone.[18,20,21] As many factors influence fracture stability, conflicting data exists.[22–25] Regardless, plate length and size are recognized as important factors in determining fracture stability and the outcome of bone healing; however, few studies have assessed structural stability as a function of plate size in ulnar fractures. Specifically, no previous studies assessed the structural stability of a lower profile, 2.7-mm plate for ulnar shaft fracture fixation compared with the current standard, 3.5-mm plate.

The purpose of this study was to quantify the biomechanical strength and stability of a composite bone model construct using 2.7-mm or 3.5-mm locking compression plates in simulated transverse and oblique fractures for fixation under (1) non-destructive cyclic axial rotation, (2) nondestructive cyclic cantilever bending, and (3) destructive cantilever bending to

failure. The underlying hypothesis was that the 2.7-mm plate would produce a different mode and location of failure while also resulting in significantly lower amounts of stress shielding in the adjacent bone and higher interfragmentary cyclic motions.

2. Methods

2.1. Materials

Twenty-one composite anatomic ulnas, designed and validated for biomechanical testing, were used (Large Ulna 3426; Sawbones, Vashon Island, WA).[26] Specimens were divided into 2 groups based on fixation construct: (1) 2.7-mm plate (N = 10) and (2) 3.5-mm plate (N = 10). One specimen was kept intact, without fixation, as a control (N = 1). Fractures were fixed with either a Synthes 2.7-mm or 3.5-mm stainless steel locking compression plate (LCP) with corresponding cortical titanium nonlocking screws (#247.374, #223.601; DePuy, Synthes, West Chester, PA). Half of the specimens in each experimental group were tested with a transverse fracture and half with an oblique fracture, for a total of 4 experimental groups of N = 5 (Fig. 1).

2.2. Specimen Preparation

Two custom cutting guides were used to create reproducible midshaft transverse (90°) and oblique (45° to the horizontal plane in the coronal plane) osteotomies, AO type 2U2A fractures. Fractures were simulated before fracture fixation with a 0.75-mm blade handsaw. Fracture fixation was performed such that no gap was visible using compression plating on transverse plates and the lag screw on oblique fractures. All fracture fixations were performed by experienced orthopaedic surgeons, using the instrumentation provided by the manufacturer. The 2.7-mm plate was 94 mm in length with 10 screw holes, and the 3.5-mm plate was 137 mm in length with 10 screw holes. All plates were placed on the medial-posterior side, using conventional dynamic compression plating techniques, with 2 screws placed proximally and 2 distally. Before bone fixation, each plate was manually contoured to achieve successful compression of the fractures. Screw placement patterns were done following the clinically accepted process of implantation for each plate. Specimens with oblique fracture patterns had an extra interfragmentary lag screw placed at 90° to the fracture line, inserted after dynamic compression plating of the fragments (Fig. 2).

After fracture fixation, a triaxial 350 Ω strain gauge rosette (FRAB-5-350-11; Tokyo Measuring Instruments Laboratory Co.) was applied to each specimen on the lateral side of the
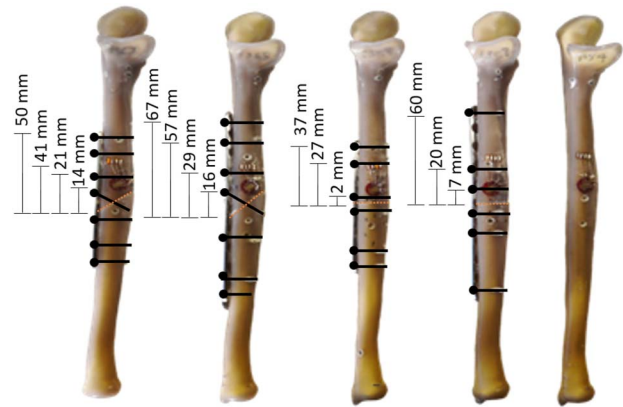

Figure 2. Test specimens with screw placement and distances from simulated reduced fractures (orange): (from left) oblique fracture with a 2.7-mm plate; oblique fracture with a 3.5-mm plate; transverse fracture with a 2.7-mm plate; transverse fracture with a 3.5-mm plate; intact ulna.

proximal fragment to measure the strain on the adjacent cortical bone near the fracture site. These measurements were used to demonstrate differences in strain between the intact, non-fractured state and the ulna constructs with either a 2.7-mm or 3.5-mm fixation. The center of the gauge was oriented 10 mm proximal to the fracture on the anterior surface. Immediately before testing, motion tracker LED flags were rigidly attached to the proximal and distal fragments to capture the relative interfragmentary translational and rotational motions using an Optotrak Certus motion tracking system (Northern Digital, Inc., Waterloo, Ontario, Canada) (Fig. 3). The motion tracking system used LED flags to track motion at specified points in space. These points were controlled on each specimen using predigitized markers at the fracture site on the proximal and distal fragments.

2.3. Experimental Loading Conditions

All specimens were tested under nondestructive conditions to simulate postoperative activities, before any destructive testing. First, specimens were tested under cyclic axial rotation, with a torsional peak of ±2 Nm, to simulate pronation and supination. Then, specimens were tested under cyclic cantilever bending in the sagittal plane, at a peak axial load of 50N (applied 200 mm from the end, resulting in a 10 Nm bending moment) to simulate posterior extension bending. Torsional loading and cantilever bending were chosen to simulate common postoperative motions, as precedented by previous fracture fixation biomechanical studies.[18,24,27,28] Finally, to assess structural stability, specimens were loaded to failure under cantilever bending at a rate of 1 mm/s[20,21]

2.4. Biomechanical Loading

All biomechanical testing was conducted using a biaxial servo-hydraulic load frame (858 Mini Bionix II; MTS Systems, Eden Prairie, MN). A force/torque load cell was used for each experiment with a capacity of 120 Nm in T_z and a 6800N capacity in F_z (F/T Sensor: Mini58; ATI Industrial Automation, Apex, NC). Axial torsion was applied through the distal end about the long axis of the ulna in the transverse plane. Free transverse translation of the proximal end was allowed using 2 linear bearings (Fig. 3b). By contrast, the distal end was fixed to an axial-torsional load cell to
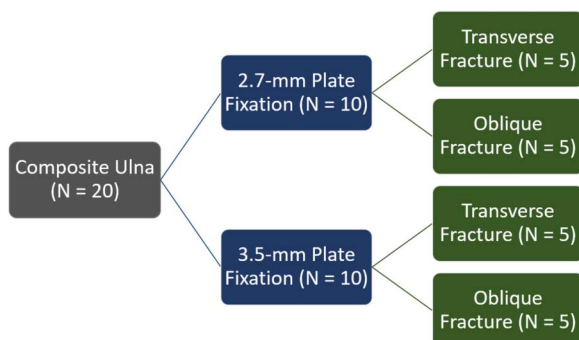

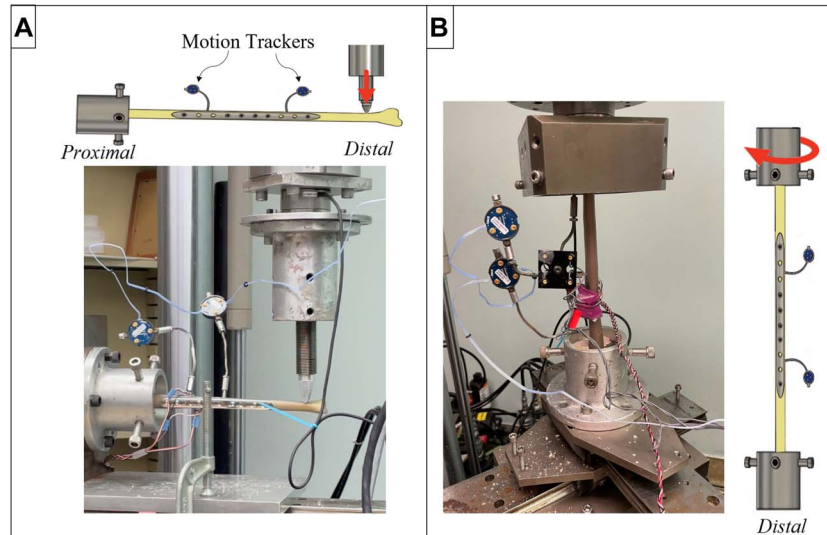**Figure 1.** Summary of relevant experimental variables.

Figure 3. Schematic and photographs of testing setup for (A) cantilever bending and (B) axial rotation.

measure the rotational moments. Cyclic axial torsion was applied with a frequency of 0.1 Hz and a peak of 2 Nm for 10 cycles.

A custom cantilever bending apparatus was fabricated. A linear force from the actuator produced the bending moment on the distal end of the ulna 200 mm from the potted proximal end. The proximal end of the ulna was rigidly fixed in the apparatus, constraining all free rotational and translational movement. The constructs were placed so the plate was most posterior (Fig. 3a). Cyclic cantilever bending was applied with a frequency of 0.25 Hz and a peak of 50N of axial load for 10 cycles.

After nondestructive cyclic loading, specimens were loaded to failure using the same cantilever bending apparatus. Two types of loading were applied for failure analysis. First, specimens were loaded at 1 mm/s until a 10-mm gap at the initial simulated fracture site was measured. Then, loading continued until ultimate failure was noted or deflection of 60 mm was achieved. Ultimate failure patterns were recorded, as well.

2.5. Data Acquisition

Triaxial rosettes were used such that the strains at 0°, 45°, and 90° from the fracture sites were measured. The magnitude and direction of the principal tensile and compressive strains were calculated for each gauge from these values. All linear and rotational motions were monitored continuously throughout nondestructive and destructive testing.

2.6. Data Collection and Statistical Analysis

Motions between the anterior edge of the ulna fracture sites were calculated using a custom MATLAB program and filtered with standard butterworth MATLAB functions (Version: R2020a; Mathworks) to calculate the average maximum motion at the fracture site. Using raw strain data from each triaxial strain gauge rosette, the principal compressive and tensile strains on the proximal end of the fracture site were calculated using an additional custom MATLAB program.

General linear models (GLMs) were constructed to determine the effects of fracture patterns and implant size on relative interfragmentary motions and principal tensile and compressive strains using

SPSS version 19.0 (IBM, Inc., Houston, TX). Within the GLMs, normality was checked for all variables by graphing the observed normal over the expected normal, and multiple comparisons were accounted for with the least significant difference test. Following the GLM to validate the models, unpaired t tests were used for specific comparisons between the 4 specimen groups.

3. Results

All specimens completed nondestructive cyclic loading under both axial rotation and cantilever bending without failure. The transverse fractures with 2.7-mm plates had the highest motion under both cyclic axial rotation (5°–10.7°) and bending (5.2 mm–6.3 mm), whereas the oblique fractures fixed with 3.5-mm plates had the least amount of motion (2.1°–3.5°; 3.2 mm–4.3 mm). The oblique fractures fixed with 2.7-mm plates created the highest strain environment 72 με −772 με) at the fracture site, and the transverse fractures fixed with 3.5-mm plates had the lowest strain environment (33 με-605 με). In destructive bending in the sagittal plane, all 3.5-mm constructs created a new peri-implant fracture at the distal screw hole, closest to the applied load; however, 4 of 5 2.7-mm constructs bent considerably, plastically deforming the plate and displacing the fracture, but did not fracture or detach at the fracture site.

3.1. Cyclic Axial Rotation

The average interfragmentary motion for the 2.7-mm constructs with oblique fractures was 5.9° ± 1.4° and for 3.5-mm constructs with oblique fractures was 3.5° ± 0.5° in nondestructive cyclic axial rotation. The average interfragmentary motion for the 2.7-mm constructs with a transverse fracture was 7.7° ± 1.9° and for the 3.5-mm constructs with a transverse fracture was 3.7° ± 1.0° (Fig. 4). Interfragmentary motion of the 2.7-mm constructs with an oblique fracture was significantly larger compared with the 3.5-mm constructs with oblique fractures ($P < 0.01$). Similarly, 2.7-mm constructs with a transverse fracture had significantly more motion than 3.5-mm constructs with transverse fractures ($P < 0.01$). No difference was seen between the 2.7-mm and 3.5-mm constructs with different fracture types ($P > 0.05$).
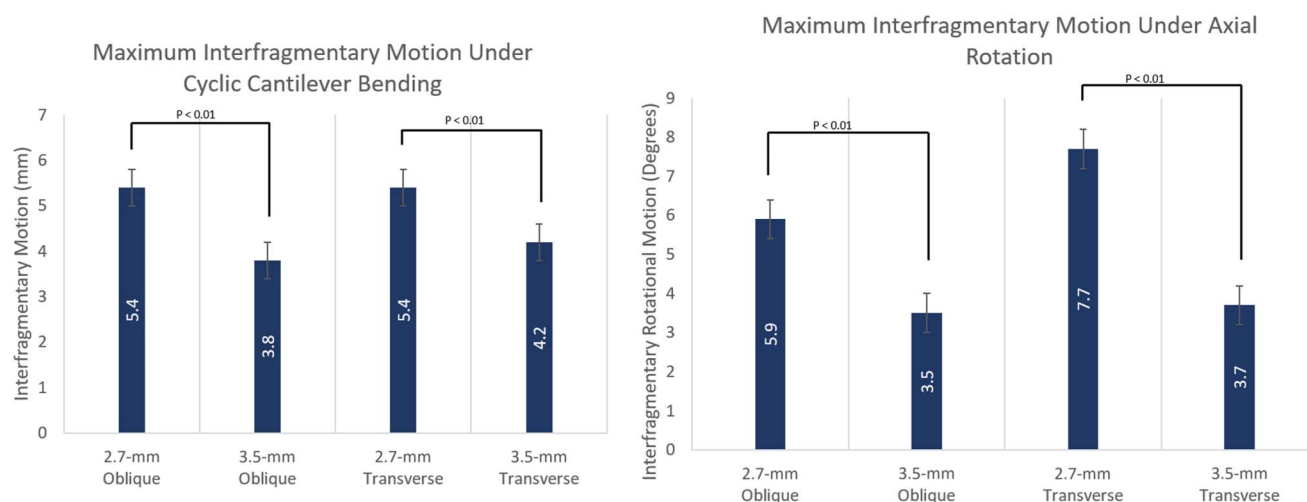
Figure 4. Comparison of experimental groups average cyclic motion in cantilever bending and axial rotation tests.

For the intact (control) specimen, all principal strains were higher than all experimental specimens, except for the 2.7-mm compressive strain in axial rotation. The intact bone had a principal tensile strain of 964 με and a principal compressive strain of 864 με. Principal compressive and tensile strains were generally comparable between all constructs, with exceptions. The 2.7-mm constructs with oblique fractures had significantly higher average principal tensile and compressive strains than the 2.7-mm constructs with transverse fractures under axial rotation ($P < 0.01$). In addition, the 2.7-mm constructs with oblique fractures had significantly higher average principal strains than the 3.5-mm constructs with oblique fractures (Fig. 5).

3.2. Cyclic Cantilever Bending

The average interfragmentary motion for the 2.7-mm constructs with oblique fractures was 5.4 ± 0.6 mm and for 3.5-mm constructs with an oblique fracture was 3.8 ± 0.35 mm in nondestructive cyclic cantilever bending. The average interfragmentary motion for the 2.7-mm constructs with a transverse fracture was 5.4 ± 0.4 mm and for the 3.5-mm constructs with a transverse fracture was 4.2 ± 0.2 mm (Fig. 4). Interfragmentary motion was significantly larger under nondestructive cantilever bending between the 2.7-mm constructs with oblique fractures compared with the 3.5-mm constructs with oblique fractures ($P < 0.01$) and significantly larger with the 2.7-mm constructs with transverse fractures compared with 3.5-mm constructs with transverse fractures ($P < 0.01$).

For the intact specimen, all principal strains were higher than all experimental specimens under nondestructive cyclic cantilever bending, with a principal tensile strain of 740 με and a principal compressive strain of 509 με. Principal compressive and tensile strains were generally comparable between all constructs, with one exception. The 2.7-mm constructs with transverse fractures had significantly higher compressive principal strain than the 3.5-mm constructs with a transverse fracture under cyclic cantilever bending (Fig. 5).

3.3. Destructive Cantilever Bending

Under destructive cantilever bending to failure, 4 of 5 of the 2.7-mm constructs with oblique fractures failed at the proximal-most screw, which experienced the highest bending moment. The remaining single specimen deformed the plate considerably but did not fracture. By contrast, 4 of 5 of the 3.5-mm constructs with oblique fractures failed at the distal-most screw, closest to the applied bending load. The remaining single specimen in this group cracked at the proximal-most screw, where the bending moment was the greatest, but did not completely fracture.

None of the 2.7-mm constructs with transverse fractures completely fractured under destructive testing. Instead, all 5 of these plates bent considerably and displaced the osteotomy but did not fracture through a screw hole as the other specimens. From this group, 2 of 5 of specimens cracked at the proximal screw hole but did not fracture completely. By contrast, all 5 of the 3.5-mm constructs with transverse fractures failed at the distal-most screw, closest to the applied load, in destructive cantilever bending.

The bending moment was calculated at the simulated fracture site for each specific construct for 10 mm of interfragmentary motion. The bending moment to create a 10-mm gap was 8.0 ± 0.5 Nm for the 2.7-mm constructs with an oblique fracture and 12.5 ± 1.4 Nm for the 3.5-mm constructs with oblique fractures ($P < 0.01$). The bending moment at the fracture site was 8.3 ± 1.1 Nm for the 2.7-mm constructs with a transverse fracture and 11.1 ± 1.1 Nm for the 3.5-mm constructs with a transverse fracture ($P = 0.01$) (Fig. 6).

Bending moments at ultimate failure were calculated at the point of refracture for each specific construct. The bending moment at ultimate failure was 32.6 ± 2.6 Nm for the 2.7-mm constructs with oblique fractures, calculated at the proximal-most screw. The bending moment at failure was 9.9 ± 2.3 Nm for the 3.5-mm constructs with oblique fractures, calculated at the distal-most screw ($P < 0.01$). The bending moment at failure was 17.9 ± 4.4 Nm for the 2.7-mm constructs with transverse fractures, calculated at the original simulated fracture site. The bending moment at ultimate failure was 10.0 ± 1.1 Nm for the 3.5-mm constructs with transverse fractures, calculated at the distal-most screw ($P < 0.01$) (Fig. 7). For the 2.7-mm constructs with an oblique fracture that did not fracture, failure was defined as deflection of 60 mm under cantilever loading at the distal (free end) without fracture.

The bending moments were calculated by multiplying the ultimate load to failure by the distance of this applied load to the point of fracture or plastic deformation of the plate. However, the 2.7-mm constructs experienced failure by bending of the
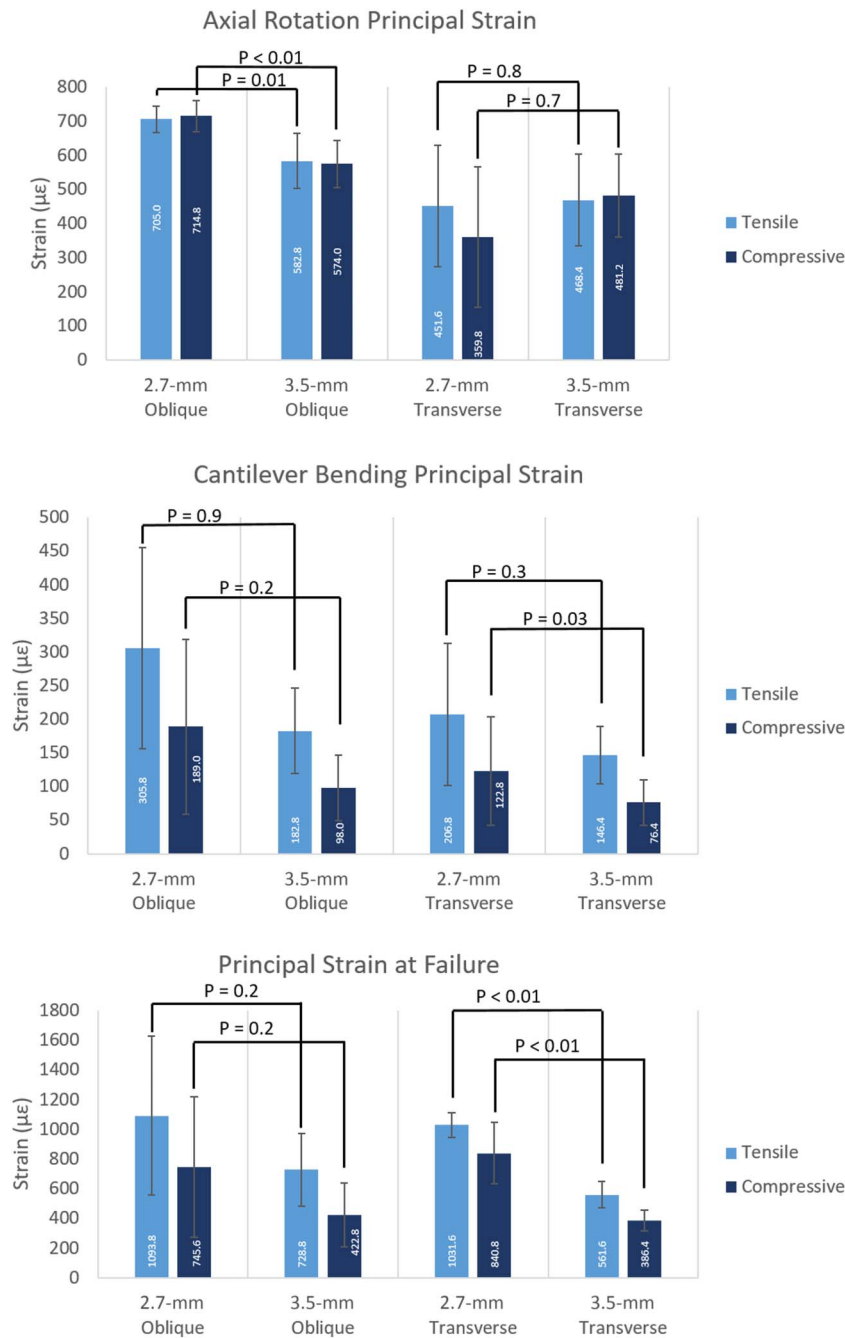
Figure 5. Principal tensile and compressive strain after torsional testing (top), cantilever bending (middle), and load to failure (bottom).

plate, resulting in opening of the fracture gap or fracture at the proximal-most screw. By contrast, the 3.5-mm constructs created a new fracture at the distal-most screw location. This discrepancy resulted in a large difference between the moment arms for the 2 constructs. For the 2.7-mm constructs with oblique fractures, ultimate load at failure was 186.5 ± 21.9N, with an average distance of 176.2 ± 14.8 mm from the point of applied load to the point of new fracture. For the 3.5-mm constructs with oblique fractures, ultimate load at failure was 171.4 ± 34.1N, with an average distance of 57.2 ± 2.3 mm from the point of applied load to the point of new fracture. For the 2.7-mm constructs with transverse fractures, ultimate load at failure was 160.3 ± 35.5N, with an average distance of 111.1

± 4.2 mm from the point of applied load to the point of new fracture. For the 3.5-mm constructs with transverse fractures, ultimate load at failure was 172.4 ± 22.4N, with an average distance of 58.1 ± 1.7 mm from the point of applied load to the point of new fracture. There was no statistical difference between the ultimate loads at failure for the 2.7-mm and 3.5-mm constructs for both oblique (P = 0.8) and transverse fractures (P = 0.6). However, the distance from the point of loading to the point of new fracture was significantly more for the 2.7-mm constructs for both oblique and transverse fractures (P < 0.001).

Interfragmentary motion and final gap distances were measured for all constructs. Specifically, of interest were the
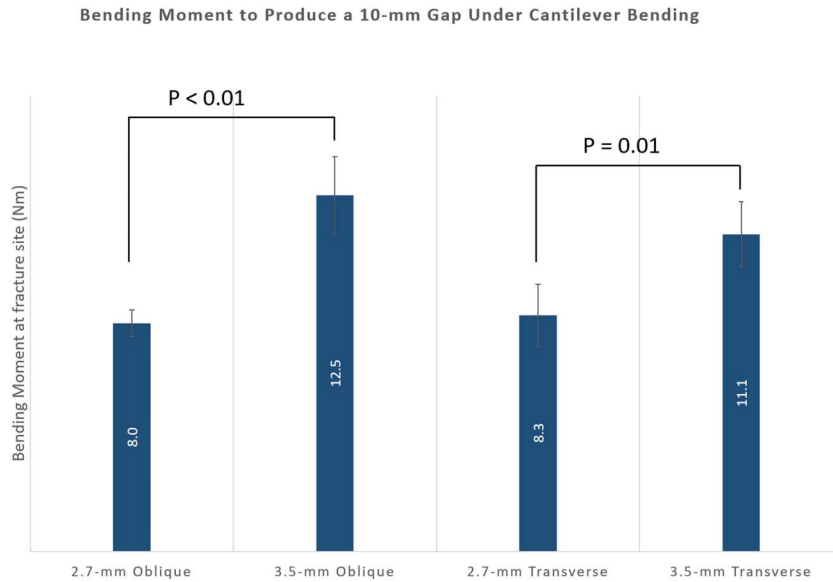
Bending Moment to Produce a 10-mm Gap Under Cantilever Bending

Figure 6. Comparison of bending moments to produce a 10-mm interfragmentary gap.

2.7-mm plates with a transverse fracture that did not produce a new ulnar fracture. The interfragmentary motion during the ultimate failure test was 34.7 ± 7.1 mm. However, the final residual gap at the simulated fracture site when the ulna completed failure testing and the load was removed was 2.4 ± 1.5 mm. This indicated that although there was plastic deformation of the constructs, there was also significant elastic deformation during testing.

4. Discussion

Despite the applied loads being larger than what would be expected during cast immobilization, the 2.7-mm plates maintained stability during nondestructive cyclic loading, showing no signs of plastic deformation. Furthermore, during destructive testing of the constructs, the flexible nature of the 2.7-mm plates continued to maintain the construct stability, compared with the 3.5 mm which fractured completely. These results indicate that the use of 2.7-mm plate may be strong enough for the period of

healing and reduce complications associated with the 3.5-mm plate, such as stress shielding and refracture rates.

Implant prominence after fixation of forearm fractures is a common complication that is associated with symptoms requiring reoperation and implant removal.[29–31] Despite the development of lower profile, smaller plates, few studies have investigated the structural stability of fixation constructs for ulnar fractures. Given the subcutaneous position of the fixation plates in the ulna, the use of smaller plates, such as the 2.7-mm LCP in this study, will reduce implant prominence.[32] Furthermore, the flexibility of these plates and the smaller size of the screw holes may be beneficial in promoting bone healing and mitigate the risk of refracture, should removal be required.[33] Currently, 3.5-mm plates are considered the standard of care for diaphyseal ulnar fracture fixation.[34–36] However, the results of this study suggest that the 2.7-mm constructs may provide some benefits for successful fracture fixation.

As expected, significant differences in both translational and rotational interfragmentary motions were seen between the 2.7-mm and 3.5-mm constructs for both transverse and oblique
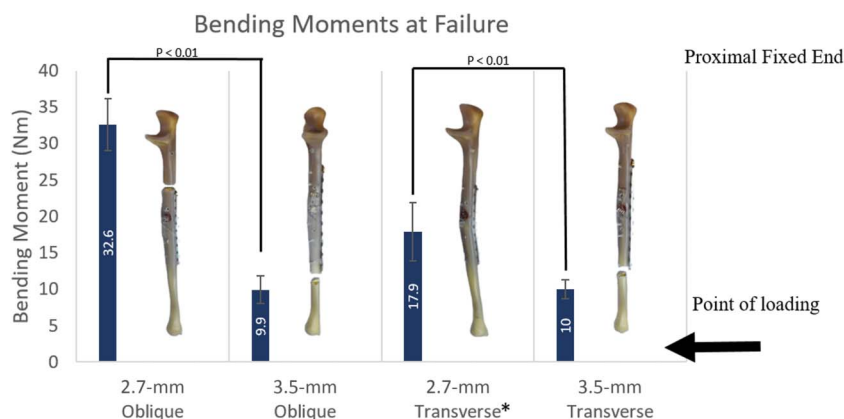

Figure 7. Comparison of representative fracture patterns with bending moments at failure showing the point of loading and fixed end. *2.7-mm plates with a transverse did not fracture, and bending moments reported are those observed at failure.

fractures. No previous studies have quantified interfragmentary motion for ulnar shaft fracture; however, studies have reported decreased motions with stiffer fracture fixation constructs in non–weight-bearing long bones.[37–39] It must be noted that other biomechanical studies have reported substantially smaller magnitudes of interfragmentary motion in axial rotation for rigidly fixed radial fractures or clavicle fractures. Specifically, the magnitudes of motions measured in this study were substantially larger, between 3.5 and 5.5 mm and 1°–4°, under cyclic bending and torsion. By contrast, Gardner et al and Zhang et al reported rotational motions of 0.035–0.05 mm in the clavicle and between 0.176 and 0.043 mm in the radius. However, it should be considered that in this study peak cyclic loading was 2 Nm of axial torsion and 10 Nm of cantilever bending, whereas Zhang et al applied a cyclic load of 0.5 Nm axial torsion and did not apply cantilever bending. The loads in this study were selected to simulate extreme physiological loading such as lifting a heavy grocery bag with the forearm in a horizontal position.[18,20,21] Furthermore, these loads did not cause plastic deformation, as indicated by the complete recovery of motion after each iteration. Clearly, these loading conditions are beyond those experienced during healing of an ulna with rigid fixation; however, they were still valid for nondestructive cyclic loading. Therefore, the higher interfragmentary motions in this study are in part due to substantially larger torsional and additional large bending moments that were applied. Furthermore, the motions in this study were reported for the edge of the fracture site between fragments at the opposite side from the plate. Because the plate is rigidly attached to both fractured segments of the ulna, only negligible axial displacement could be expected at this edge. Contrarily, on the opposite edge from the plate maximum separation and interfragmentary displacement may be expected from plate deformation and bending. In addition, the motions were measured with no soft-tissue support, whereas, in reality, loads in the forearm would be shared with the radius through the interosseous membrane and the distal and proximal radioulnar joints. Nevertheless, the motions measured in this study, although exaggerated, serve to highlight the relative differences in mechanism of loading and potential failure between the 2 plate sizes.

Despite the 3.5-mm construct being effective in preventing motion, the stiffness of the plate may be larger than necessary leading to the larger amounts of stress shielding.[40] The buildup of stresses can lead to a small region of the bone, a stress concentration, in which the system will fail more readily than if the plate can successfully disperse forces. High stresses can cause stress risers at the end screws or near the fracture site.[33,41–43] In this study's model, a force was applied on the distal portion of the ulna, potentially resulting in a stress concentration at the weakest point between the end of the fracture plate and the unprotected bone or the most distal screw. Accordingly, the majority of the 3.5-mm constructs fractured completely through the distal-most screw and at a significantly smaller bending moment, less than 12 Nm (Fig. 7). By contrast, the 2.7-mm constructs were able to withstand a larger bending moment of more than 30 Nm before fracturing, and when peri-implant fractures were observed, it was at the proximal-most screw where the bending moment was the largest. As such, the bending moment for all 3.5-mm plates at ultimate failure was much smaller than the 2.7-mm plates because the distance from the applied load to the point of failure was significantly less for the 3.5-mm constructs compared with the 2.7-mm constructs. These observations suggested that a considerable stress concentration was applied at the distal-most screw following sagittal plane bending loads for 3.5-mm constructs.[18,44] In addition, none of the

2.7-mm constructs with a transverse fracture completely detached. Instead, the plate bent considerably, plastically deforming, and displaced the fracture. One possible explanation for this observation may be that the 2.7 mm allowed for forces to be dissipated throughout the plate, diminishing a stress concentration at one screw, potentially decreasing the incidence of refractures. Although the ultimate failure loads may not be clinically relevant, loading to failure beyond the 10-mm gap deformation provided valuable insight for locations of stress concentrations and potential modes of failure in the event of trauma. This indicates that the use of 2.7-mm plate may reduce the risk of peri-implant refracture in the event of repeat trauma.

Furthermore, in clinical use, a larger size and highly rigid fixation plate in weight-bearing long bones has been shown to compromise bone healing and result in a higher degree of cortical porosity.[45–50] This, depending on the time allowed for fracture healing, may potentially result in another peri-implant fracture. Studies regarding femoral fracture fixation have shown that an increase in rigidity of fixation can be problematic to secondary healing and cause failure of the device.[33,51] Acknowledging the differences between weight-bearing and non–weight-bearing fracture healing and fixation, specifically the absolute stability typically necessary in the forearm, the breadth of the literature surrounding fracture healing in weight-bearing bones is more extensive than for non–weight-bearing joints and is a good resource for exploring potential complications and associated caution. In this literature, the use of larger compression plates has been reported to result in higher refracture rates on removal.[10,52] This could be due to a stress riser at the original fracture site following implant removal because of insufficient bone growth and blood supply.[39] Furthermore, fractures may also occur through residual screw holes. This could indicate that, a less-rigid, smaller fracture fixation plate with smaller screws, such as the 2.7-mm plate, may reduce the presence of stress risers while promoting bone healing.[53]

In this study, in addition to the measurement of interfragmentary motion, principal compressive and tensile strains on the cortical bone adjacent to the fracture site were measured.[54] Both the 2.7-mm and 3.5-mm constructs produced substantially lower magnitudes of principal strain than the intact ulna under the same loading conditions. Based on the results of this study, the 2.7-mm constructs produced generally equivalent or higher strains than the 3.5-mm constructs under both axial rotation and sagittal cantilever bending. These findings were generally consistent with biomechanical principles of plate fixation where the rigidity of the plate is directly correlated to the extent of stress shielding within bone. These results suggest that there was adequate load sharing from both plates in the immediate postoperative period to promote secondary bone healing with compression plating. In addition, the 2.7-mm constructs may provide a potential advantage for promotion of fracture healing by producing a lower magnitude of strain shielding.[22–25,55] Maintaining low strain at the fracture site is critical for primary fracture healing; however, rigid fixation that minimizes motion will prevent callus formation.[56]

4.1. Limitations

Limitations of this study include the use of a biomechanical composite ulna model. A composite model was chosen to minimize specimen variability, increase precision in detecting differences between constructs and decrease time-sensitivity. Motion is an important factor in understanding whether a smaller fixation plate may be advantageous; however, there are many other factors

influencing fracture site motion that were not replicated in this biomechanical study which may be critical in controlling motion. Furthermore, the strain gauges were placed on the lateral side of the bone because of size constraints which may have resulted in lower strains during cantilever bending because this placement was closer to the bone's neutral zone. This study does not account for the initial period of postoperative immobilization which may allow for some bone growth and fixation to decrease motions seen at the fracture site.

5. Conclusion

The 3.5-mm plates maintained greater stability throughout the nondestructive testing and successfully limited interfragmentary motion significantly more than the 2.7-mm plates. Regardless, the 2.7-mm plates maintained stability throughout nondestructive testing, exhibiting no plastic deformation. Furthermore, the difference between the ultimate load at failure was not significant between the 2.7-mm and 3.5-mm plates for either fracture; however, the distance from the point of loading to the point of new fracture was significantly less for the 3.5-mm plates. Under destructive testing, the 2.7-mm plates allowed for a larger bending moment before failure, with failure occurring in the proximal-most screw or at the fracture site. By contrast, the 3.5-mm plates failed significantly more abruptly with lower bending moments because of the difference in the moment arm. This may indicate that the 2.7-mm plates have some potential benefits, because of their increased flexibility, such as decreased stress shielding and the potential to decrease the incidence of refractures.

REFERENCES

1. Patel DS, Statuta SM, Ahmed N. Common fractures of the radius and ulna. *Am Fam Physician*. 2021;103:345–354.
2. Chung KC, Spilson SV. The frequency and epidemiology of hand and forearm fractures in the United States. *J Hand Surg*. 2001;26:908–915.
3. Sauder DJ, Athwal GS. Management of isolated ulnar shaft fractures. *Hand Clin*. 2007;23:179–184.
4. Anderson LD, Sisk D, Tooms RE, et al. Compression-plate fixation in acute diaphyseal fractures of the radius and ulna. *J Bone Joint Surg Am*. 1975;57:287-297.
5. Al-Sadek TA, Niklev D, Al-Sadek A. Diaphyseal fractures of the forearm in adults, plating or intramedullary nailing is a better option for the treatment? *Open Access Maced J Med Sci*. 2016;4:670–673.
6. Egol KA, Kubiak EN, Fulkerson E, et al. Biomechanics of locked plates and screws. *J Orthop Trauma*. 2004;18:488–493.
7. Claes L. Biomechanical principles and mechanobiologic aspects of flexible and locked plating. *J Orthop Trauma*. 2011;25(suppl 1):S4–S7.
8. Schulte LM, Meals CG, Neviaser RJ. Management of adult diaphyseal both-bone forearm fractures. *J Am Acad Orthop Surg*. 2014;22:437–446.
9. Richards TA, Deal DN. Distal ulna fractures. *J Hand Surg*. 2014;39:385–391.
10. Chapman MW, Gordon JE, Zissimos AG. Compression-plate fixation of acute fractures of the diaphyses of the radius and ulna. *J Bone Joint Surg Am*. 1989;71:159–169.
11. Hertel R, Pisan M, Lambert S, et al. Plate osteosynthesis of diaphyseal fractures of the radius and ulna. *Injury*. 1996;27:545–548.
12. Kessler SB, Deiler S, Schiffl-Deiler M, et al. Refractures: a consequence of impaired local bone viability. *Arch Orthop Trauma Surg*. 1992;111:96–101.
13. Jones DB, Jr., Kakar S. Adult diaphyseal forearm fractures: intramedullary nail versus plate fixation. *J Hand Surg*. 2011;36:1216–1219.
14. Mih AD, Cooney WP, Idler RS, et al. Long-term follow-up of forearm bone diaphyseal plating. *Clin Orthop Relat Res*. 1994:256–258.
15. Vopat BG, Kane PM, Fitzgibbons PG, et al. Complications associated with retained implants after plate fixation of the pediatric forearm. *J Orthop Trauma*. 2014;28:360–364.
16. Deluca PA, Lindsey RW, Ruwe PA. Refracture of bones of the forearm after the removal of compression plates. *J Bone Joint Surg Am*. 1988;70:1372–1376.
17. Yao C-K, Lin K-C, Tarng Y-W, et al. Removal of forearm plate leads to a high risk of refracture: decision regarding implant removal after fixation of the forearm and analysis of risk factors of refracture. *Arch Orthop Trauma Surg*. 2014;134:1691–1697.
18. Collins M, Hart A, Hines J, et al. Distal ulna fractures: a biomechanical comparison of locking versus nonlocking plating constructs. *J Orthop Trauma*. 2014;28:470–475.
19. Uhthoff HK, Poitras P, Backman DS. Internal plate fixation of fractures: short history and recent developments. *J Orthop Sci*. 2006;11:118–126.
20. Fulkerson E, Egol KA, Kubiak EN, et al. Fixation of diaphyseal fractures with a segmental defect: a biomechanical comparison of locked and conventional plating techniques. *J Trauma*. 2006;60:830–835.
21. Sanders R, Haidukewych GJ, Milne T, et al. Minimal versus maximal plate fixation techniques of the ulna: the biomechanical effect of number of screws and plate length. *J Orthop Trauma*. 2002;16:166–171.
22. Müller M. Theoretical and practical principles of rigid internal fixation. In: *Technique of Internal Fixation of Fractures*. Berlin, Heidelberg: Springer; 1965, pp 7–19.
23. Müller ME, Perren SM, Allgöwer M, et al. *Manual of Internal Fixation: Techniques Recommended by the AO-ASIF Group*. Berlin, Heidelberg: Springer Science & Business Media; 1991.
24. Hopf JC, Mehler D, Nowak TE, et al. Nailing of diaphyseal ulna fractures in adults-biomechanical evaluation of a novel implant in comparison with locked plating. *J Orthop Surg Res*. 2020;15:158.
25. McKibbin B. The biology of fracture healing in long bones. *J Bone Joint Surg Br*. 1978;60:150–162.
26. Kennedy JG, Carter DR. Long bone torsion: I. Effects of heterogeneity, anisotropy and geometric irregularity. *J Biomech Eng*. 1985;107:183–188.
27. Chiu Y-C, Hsu C-E, Ho T-Y, et al. Biomechanical study on fixation methods for horizontal oblique metacarpal shaft fractures. *J Orthop Surg Res*. 2022;17:374.
28. Strauss EJ, Banerjee D, Kummer FJ, et al. Evaluation of a novel, nonspanning external fixator for treatment of unstable extra-articular fractures of the distal radius: biomechanical comparison with a volar locking plate. *J Trauma*. 2008;64:975–981.
29. Bugarinovic G, McFarlane KH, Benavent KA, et al. Risk factors for hardware-related complications after olecranon fracture fixation. *Orthopedics*. 2020;43:141–146.
30. Nemeth N, Bindra RR. Fixation of distal ulna fractures associated with distal radius fractures using intrafocal pin plate. *J Wrist Surg*. 2014;3:55–59.
31. Perdue PW, Satalich J, Jauregui J. Complications and risk factors influencing hardware removal after open reduction and internal fixation of the radius or ulna: a nationwide study. *J Long Term Eff Med Implants*. 2020;30:49–55.
32. Park HY, Kim SJ, Sur YJ, et al. Refracture after locking compression plate removal in displaced midshaft clavicle fractures after bony union: a retrospective study. *Clin Shoulder Elbow*. 2021;24:72–79.
33. Graham SM, Moazen M, Leonidou A, et al. Locking plate fixation for Vancouver B1 periprosthetic femoral fractures: a critical analysis of 135 cases. *J Orthop Sci*. 2013;18:426–436.
34. Leung F, Chow SP. A prospective, randomized trial comparing the limited contact dynamic compression plate with the point contact fixator for forearm fractures. *J Bone Joint Surg Am*. 2003;85:2343–2348.
35. Leung F, Chow SP. Locking compression plate in the treatment of forearm fractures: a prospective study. *J Orthop Surg (Hong Kong)*. 2006;14:291–294.
36. Ling HT, Kwan MK, Chua YP, et al. Locking compression plate: a treatment option for diaphyseal nonunion of radius or ulna. *Med J Malaysia*. 2006;61(suppl B):8–12.
37. Zhang Y, Shao Q, Yang C, et al. Finite element analysis of different locking plate fixation methods for the treatment of ulnar head fracture. *J Orthop Surg Res*. 2021;16:191.
38. Pulos N, Yoon RS, Shetye S, et al. Anteroinferior 2.7-mm versus 3.5-mm plating of the clavicle: a biomechanical study. *Injury*. 2016;47:1642–1646.
39. Gardner MJ, Brophy RH, Campbell D, et al. The mechanical behavior of locking compression plates compared with dynamic compression plates in a cadaver radius model. *J Orthop Trauma*. 2005;19:597–603.
40. Alexander J, Morris RP, Kaimrajh D, et al. Biomechanical evaluation of periprosthetic refractures following distal femur locking plate fixation. *Injury*. 2015;46:2368–2373.

41. Buttaro M, Farfalli G, Núñez MP, et al. Locking compression plate fixation of Vancouver type-B1 periprosthetic femoral fractures. *J Bone Joint Surg Am*. 2007;89:1964–1969.

42. Ebraheim NA, Gomez C, Ramineni SK, et al. Fixation of periprosthetic femoral shaft fractures adjacent to a well-fixed femoral stem with reversed distal femoral locking plate. *J Trauma Acute Care Surg*. 2009;66: 1152–1157.

43. Tsiridis E. Authors' Reply-Dall-Miles plates for periprosthetic femoral fractures a critical review of 16 cases. *Injury*. 2004;35:440–441.

44. Stoffel K, Dieter U, Stachowiak G, et al. Biomechanical testing of the LCP–how can stability in locked internal fixators be controlled? *Injury*. 2003; 34(suppl 2):B11–B19.

45. Claes L. The mechanical and morphological properties of bone beneath internal fixation plates of differing rigidity. *J Orthop Res*. 1989;7: 170–177.

46. Gardner MJ, Evans JM, Dunbar RP. Failure of fracture plate fixation. *J Am Acad Orthop Surg*. 2009;17:647–657.

47. Perren SM. Evolution of the internal fixation of long bone fractures: the scientific basis of biological internal fixation: choosing a new balance between stability and biology. *J Bone Joint Surg Br*. 2002;84: 1093–1110.

48. Patel R, Neu CP, Curtiss S, et al. Crutch weightbearing on comminuted humeral shaft fractures: a biomechanical comparison of large versus small fragment fixation for humeral shaft fractures. *J Orthop Trauma*. 2011;25: 300–305.

49. Ganesh V, Ramakrishna K, Ghista DN. Biomechanics of bone-fracture fixation by stiffness-graded plates in comparison with stainless-steel plates. *Biomed Eng Online*. 2005;4:1–15.

50. Akeson W, Woo S, Coutts R, et al. Quantitative histological evaluation of early fracture healing of cortical bones immobilized by stainless steel and composite plates. *Calcif Tissue Res*. 1975;19:27–37.

51. Moazen M, Jones AC, Jin Z, et al. Periprosthetic fracture fixation of the femur following total hip arthroplasty: a review of biomechanical testing. *Clin Biomech*. 2011;26:13–22.

52. Beaupré GS, Csongradi JJ. Refracture risk after plate removal in the forearm. *J Orthop Trauma*. 1996;10:87–92.

53. Hart NH, Nimphius S, Rantalainen T, et al. Mechanical basis of bone strength: influence of bone material, bone structure and muscle action. *J Musculoskelet Neuronal Interact*. 2017;17:114.

54. Ziran N, McCarty CP, Ho NC, et al. A novel intramedullary nail to control interfragmentary motion in diaphyseal tibial fractures. *J Orthop Res*. 2022;40:1053–1064.

55. Jagodzinski M, Krettek C. Effect of mechanical stability on fracture healing–an update. *Injury*. 2007;38(suppl 1):S3–S10.

56. Hak DJ, Toker S, Yi C, et al. The influence of fracture fixation biomechanics on fracture healing. *Orthopedics*. 2010;33:752–755.